

## Tuning the ferromagnetic-antiferromagnetic interfaces of granular Co-CoO exchange bias systems by annealing

E. Menéndez, H. Modarresi, T. Dias, J. Geshev, L. M. C. Pereira, K. Temst, and A. Vantomme

Citation: *Journal of Applied Physics* **115**, 133915 (2014); doi: 10.1063/1.4870713

View online: <http://dx.doi.org/10.1063/1.4870713>

View Table of Contents: <http://scitation.aip.org/content/aip/journal/jap/115/13?ver=pdfcov>

Published by the [AIP Publishing](#)

---

### Articles you may be interested in

[Enhancement of the magnetic interfacial exchange energy at a specific interface in NiFe/CoO/Co trilayer thin films via ion-beam modification](#)

*J. Appl. Phys.* **115**, 073901 (2014); 10.1063/1.4865569

[Improvement of magnetic particle stability upon annealing in an exchange-biased nanogranular system](#)

*J. Appl. Phys.* **100**, 064312 (2006); 10.1063/1.2338134

[Domain formation in exchange biased Co/CoO bilayers](#)

*J. Appl. Phys.* **93**, 7726 (2003); 10.1063/1.1540152

[Tuning exchange bias](#)

*Appl. Phys. Lett.* **75**, 2304 (1999); 10.1063/1.124998

[Spin wave frequency shifts in exchange coupled ferromagnet/antiferromagnet structures: Application to Co/CoO](#)

*J. Appl. Phys.* **81**, 4485 (1997); 10.1063/1.364986

---



**Not all AFMs are created equal**  
**Asylum Research Cypher™ AFMs**  
**There's no other AFM like Cypher**

[www.AsylumResearch.com/NoOtherAFMLikeIt](http://www.AsylumResearch.com/NoOtherAFMLikeIt)

**OXFORD**  
INSTRUMENTS  
*The Business of Science®*

# Tuning the ferromagnetic-antiferromagnetic interfaces of granular Co-CoO exchange bias systems by annealing

E. Menéndez,<sup>1,a)</sup> H. Modarresi,<sup>1</sup> T. Dias,<sup>1,2</sup> J. Geshev,<sup>2</sup> L. M. C. Pereira,<sup>1</sup> K. Temst,<sup>1</sup> and A. Vantomme<sup>1</sup>

<sup>1</sup>Instituut voor Kern- en Stralingsfysica, KU Leuven, Celestijnenlaan 200 D, BE-3001 Leuven, Belgium

<sup>2</sup>Instituto de Física, Universidade Federal do Rio Grande do Sul (UFRGS), Porto Alegre, 91501-970 Rio Grande do Sul, Brazil

(Received 13 February 2014; accepted 26 March 2014; published online 7 April 2014)

The low-temperature magnetic behavior of granular Co-CoO exchange bias systems, prepared by oxygen ion implantation in Co thin films and subsequent annealing, is addressed. The thermal activation effects lead to an O migration which results in virtually pure Co areas embedded in a structurally relaxed and nearly stoichiometric CoO phase. This yields decreased training and exchange bias shifts, while the blocking temperature significantly increases, coming close to the Néel temperature of bulk CoO for samples implanted to a fluence above  $1 \times 10^{17}$  ions/cm<sup>2</sup> (15% O). The dependence of the exchange bias shift on the pristine O-implanted content is analogous to that of the antiferromagnetic thickness in most ferromagnetic/antiferromagnetic systems (i.e., an increase in the exchange bias shift up to a maximum followed by a decrease until a steady state is reached), suggesting that, after annealing, the enriched Co areas might be rather similar in size for samples implanted above  $1 \times 10^{17}$  ions/cm<sup>2</sup>, whereas the corresponding CoO counterparts become enlarged with pristine O content (i.e., effect of the antiferromagnet size). This study demonstrates that the magnetic properties of granular Co-CoO systems can be tailored by controllably modifying the local microstructure through annealing treatments. © 2014 AIP Publishing LLC. [<http://dx.doi.org/10.1063/1.4870713>]

## I. INTRODUCTION

Exchange bias (EB)<sup>1–4</sup> is an interfacial phenomenon which commonly arises from the magnetic exchange coupling between a ferromagnet (FM) and an antiferromagnet (AFM).<sup>5,6</sup> This is typically initiated by field cooling the system below the Néel temperature of the AFM, usually resulting in a shift along the field axis ( $H_E$ ) and a coercivity,  $H_C$ , enhancement.<sup>1–4</sup> EB systems often exhibit the so-called training effect (i.e., the degradation of the exchange bias shift with consecutively measured hysteresis loops).<sup>1–4,7–11</sup> The ongoing demand to overcome scaling barriers in *spintronics*<sup>12,13</sup> together with the interest in fundamental properties directly related to the low dimensionality (i.e., finite size effects) continue to drive the development of advanced magnetic nanostructures with precisely controlled properties, propelling a renewed interest in exchange-biased nanostructures where thermal stability is a crucial aspect to face potential applications.<sup>3</sup> The majority of EB research has been focused on thin films, with Co-CoO bilayers constituting a valuable model system.<sup>14</sup> Alternatively, ion implantation has been demonstrated to be a suitable approach to control the EB properties of granular-like FM-AFM systems with multiple interfaces, such as Co-CoO<sup>15–18</sup> or Ni-NiO.<sup>18</sup> Recently, by the interplay between implantation conditions and sample design, it has been shown that the O-depth profile across the FM layer thickness can be controlled using a single-energy ion implantation approach.<sup>17</sup> In particular, in contrast to both bilayers and FM films with a Gaussian-like

O-depth profile, uniform O-depth distributions result in superior low-temperature EB properties, such as enhanced exchange-coupling strength, improved loop homogeneity or increased blocking temperature ( $T_B$ ). However, the behavior of such granular systems under thermal-activation effects still remains unexplored. In this paper, we present a detailed study of the role of annealing effects in the EB properties of O-implanted Co thin films with a uniform O-depth profile.

## II. EXPERIMENTAL

Polycrystalline samples consisting of a Au capping layer (15 or 30 nm)/Co layer (30 nm)/Au buffer layer (10 nm)/SiO<sub>2</sub> (500 nm)/Si (100) were grown by molecular beam epitaxy.<sup>17</sup> 40 keV O ions and fluences of  $3 \times 10^{16}$ ,  $5 \times 10^{16}$ ,  $1 \times 10^{17}$ , and  $2 \times 10^{17}$  ions/cm<sup>2</sup> were used to implant the samples with a 15 nm thick Au capping layer, while samples with a 30 nm thick Au capping layer were implanted to  $3.25 \times 10^{17}$  and  $5.5 \times 10^{17}$  ions/cm<sup>2</sup> using 50 keV O ions. As previously shown,<sup>17,19</sup> these conditions give rise to a relatively uniform O depth distribution along the Co layer with an atomic O concentration of around 5%, 8%, 15%, 26%, 34%, and 44%, respectively. Subsequently, with the aim to moderately promote thermal activation while avoiding a pronounced transformation of the system (e.g., due to full recrystallization), the samples were annealed in vacuum (pressure  $< 1 \times 10^{-6}$  millibars) at 300 °C (a temperature which is well below the bulk melting points of the diverse constituents) for 1 h. In order to avoid any type of quenching-related effects, the heating and cooling rates were set to be rather slow (i.e., 5 °C/min). From a structural point of view, the samples were

<sup>a)</sup>Electronic mail: Enric.MenendezDalmau@fys.kuleuven.be

characterized by transmission electron microscopy (TEM). High-angle annular dark-field imaging in scanning TEM mode was used to identify the main composition of the diverse structural features. Further, synchrotron grazing incidence X-ray diffraction (GIXRD) at an angle of  $1.5^\circ$  using a wavelength of  $1.199 \text{ \AA}$  was also carried out. The GIXRD measurements were performed at the Rossendorf (Helmholtz Zentrum Dresden-Rossendorf) BM20 beamline at the European Synchrotron Radiation Facility (ESRF). Superconducting quantum interference device (SQUID) magnetometry was used to magnetically study the low-temperature (10 K) EB properties after field cooling the samples from room temperature in an in-plane applied magnetic field of 400 mT. Training effects were investigated by measuring consecutive SQUID hysteresis loops until equilibrium (i.e., saturation of the EB shift) was reached. To estimate  $T_B$ , hysteresis loops were measured as a function of temperature starting from a fully trained state.

### III. RESULTS AND DISCUSSION

As can be seen in Fig. 1(a), the as-deposited sample implanted to  $3.25 \times 10^{17} \text{ ions/cm}^2$  exhibits an O-rich Au phase at the interface between the capping and the Co layer. Conversely, the annealed film shows a partial recovery of the layer stack (i.e., Au/Co/Au), indicating that the thermal activation favors O migration towards the surface of the Au capping layer. This is in agreement with previously reported studies, which report on the role of surface effects in increasing the limited O solubility in Au.<sup>20</sup> A similar phenomenon might also apply for Co (i.e., separation of O and Co), since a pronounced contrast is observed in the Co layer itself. However, the prone nature of Co to rapidly oxidize may

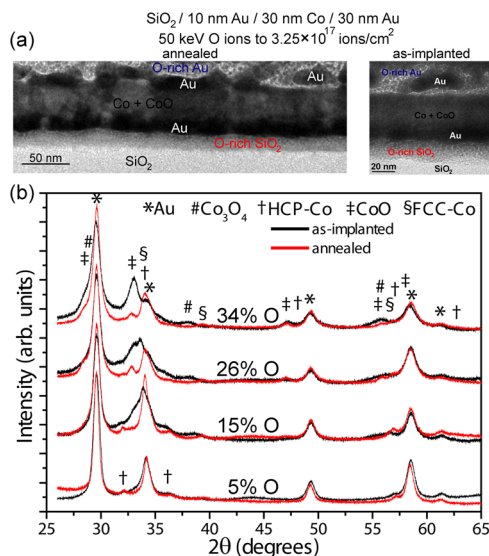


FIG. 1. (a) TEM images of a cross section of the sample implanted to a fluence of  $2 \times 10^{17} \text{ ions/cm}^2$  and annealed (left) and the corresponding as-implanted film (right). (b) Synchrotron grazing incidence X-ray diffraction patterns of different as-implanted<sup>19</sup> and annealed samples. The main peaks of Au (64701-ICSD—Inorganic Crystal Structure Database), HCP-Co (76633-ICSD), CoO (29049-ICSD), and FCC-Co (76632-ICSD) are indicated in the figure. Since weak traces of  $\text{Co}_3\text{O}_4$  (28158-ICSD) are observed, only the main peaks of  $\text{Co}_3\text{O}_4$  are labeled.<sup>21</sup>

partially hinder this effect under TEM characterization since sample preparation involves natural oxidation. Synchrotron GIXRD was also performed to further investigate the role of thermal-assisted effects in the morphology and structure of the films. Fig. 1(b) shows a direct comparison between previously reported GIXRD patterns corresponding to the as-implanted films<sup>19</sup> and those of the annealed samples. It is worth noting that the annealing does not result in new phases. Besides the perceptible sharpening of the Au peaks due to both structural relaxation and grain growth (i.e., O migration to surface), the annealed samples exhibit patterns with enlarged HCP-Co and FCC-Co XRD peaks (more pronounced in patterns (i) and (ii) since the pristine amount of metallic Co is larger). This is in concordance with the TEM results, evidencing an annealing induced phase separation process in the O-implanted Co layer which leaves virtually pure Co areas. Moreover, a strong reduction of the CoO peaks and an almost full dissolution of the  $\text{Co}_3\text{O}_4$  peaks is also observed, suggesting that O partially diffuses away from the Co layer. This reduction in the amount of CoO can be qualitatively estimated by comparing the relative intensities between the (200) CoO peak (located around  $33.0^\circ$  and  $32.8^\circ$  for the as-implanted and annealed samples, respectively) and the (111) Au peak (located around  $29.6^\circ$  for either the as-implanted or annealed films). For instance, this yields values of 30.8% and 9.4% for the sample implanted at  $2 \times 10^{17} \text{ ions/cm}^2$  and the corresponding annealed one, respectively. In addition, the signal-to-noise ratio of the GIXRD patterns slightly improves after annealing, confirming the induced structural relaxation and the increase of the amount of crystalline phases in detriment of defective parts, such as grain boundaries or interfaces.

Figures 2(a)–2(d) show the consecutive SQUID measurements at 10 K corresponding to the films implanted at  $3 \times 10^{16}$ ,  $1 \times 10^{17}$ ,  $2 \times 10^{17}$ , and  $5.5 \times 10^{17} \text{ ions/cm}^2$  and annealed, respectively. Similar to the magnetometry results of the as-implanted samples,<sup>17,19</sup> the loops are still rather symmetric and characterized by sharp descending and ascending branches, indicating that magnetization inversion takes place at well-defined switching fields, thus confirming the homogeneity of the formed CoO profile along the Co layer even after annealing. Nonetheless, contrary to the as-implanted samples, training extends over a lower number of consecutively measured hysteresis loops, thus stabilizing faster. For instance, while the sample implanted at  $2 \times 10^{17} \text{ ions/cm}^2$  (26% O) needs 8 consecutive hysteresis loops to level off the EB shift, only 5 cycles are required after annealing (Fig. 2(c)). Furthermore, while the steepness remains rather unaltered, the relative training<sup>17</sup> values become strongly reduced after annealing. Namely, while the samples implanted at  $5 \times 10^{16}$  and  $5.5 \times 10^{17} \text{ ions/cm}^2$  exhibit relative training values of 68.7% and 29.9%,<sup>17,19</sup> the annealing causes a pronounced reduction down to 30.7% and 17.5%, respectively. In agreement with the structural characterization, this is in line with a CoO phase with improved stoichiometry, less prone to size effects and increased magnetocrystalline anisotropy, which ultimately establishes better defined magnetic easy axes (inhibiting other ones) and, thus, reducing training.<sup>17,19,22–25</sup> Since annealing results

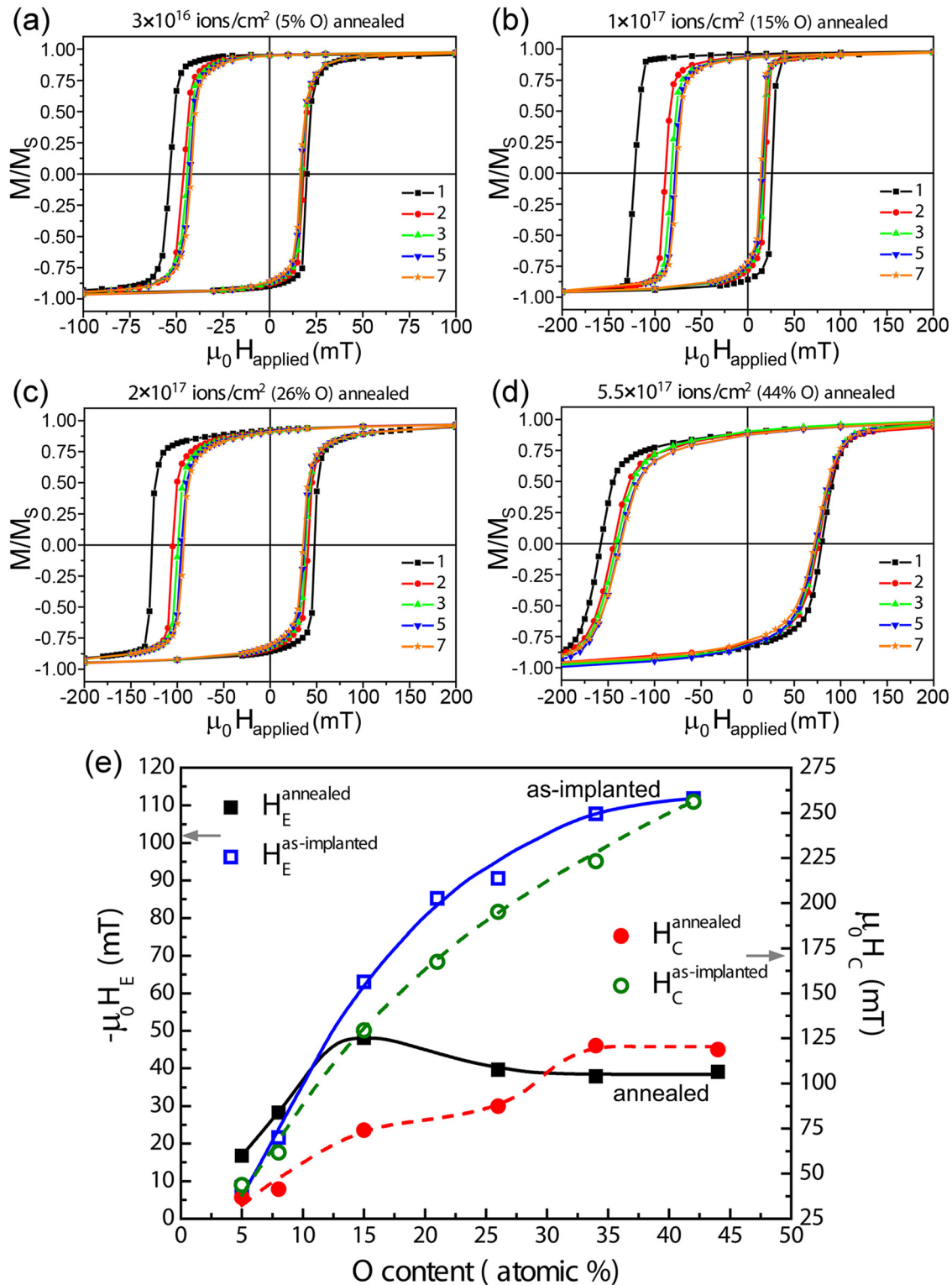


FIG. 2. (a)–(d) are the consecutive SQUID measurements at 10K after field cooling from room temperature for the films implanted at  $3 \times 10^{16}$  (5% O),  $1 \times 10^{17}$  (15% O),  $2 \times 10^{17}$  (26% O), and  $5.5 \times 10^{17}$  ions/cm<sup>2</sup> (44% O) and annealed, respectively. (e) Dependencies of the exchange bias shift,  $H_E$ , and coercivity,  $H_C$ , as a function of the implanted O content for the as-implanted<sup>17</sup> and the annealed samples. The lines in (a)–(d) are connections between the data and, in (e), guides to the eye.

in a structural relaxation (where a narrower distribution of structural defects is expected), the additional interfacial morphology training on top of that already known to arise from the AFM magnetic symmetry might be rather minimized, thus stabilizing training faster.<sup>8</sup> Further, as can be seen in

Fig. 2(e), the thermal treatment leads to decreased EB shifts and coercivities with respect to the as-implanted samples.<sup>17,19</sup> This decrease in  $H_E$  and  $H_C$  might be mainly ascribed to the decreased number of FM/AFM interfaces since annealing promotes phase separation.<sup>16,17</sup> Moreover, in

the framework of the domain state model,<sup>26</sup> annealing may result in an AFM CoO with decreased volume domains which negatively influence EB. This decrease could also be related to the size increase of the Co regions, as evidenced in the structural analysis. Given that  $H_E$  is inversely proportional to the size of the FM constituent,<sup>1-4</sup> any increase in the Co size should bring about a reduction of  $H_E$ . In this context, although the  $H_E$  dependence on the AFM thickness can be rather complex,<sup>1,3</sup> it is worth noting that the dependence of the EB shift on the pristine implanted O content for the annealed samples resembles that of the AFM thickness in FM/AFM systems. For the annealed films, with increasing oxygen content, an increase in the magnitude of the exchange bias shift up to a maximum followed by a decrease towards a steady state is observed.<sup>3,27</sup> Similar behavior (i.e., peak of  $H_E$  as a function of the AFM thickness) has already been reported in other systems, such as Co (8 nm)/CoO<sup>25</sup> bilayers, Co (4 nm)/Cu (2.3 nm)/Co (2.6 nm)/Ir<sub>25</sub>Mn<sub>75</sub> layered spin valves<sup>28</sup> or powdered SrFe<sub>12</sub>O<sub>19</sub> coated with different thicknesses of CoO.<sup>29</sup> Even though the CoO forms at the expense of the Co grain size in the as-implanted samples, this might not be applicable to the annealed specimens since O migration away from Co occurs noticeably. However, taking into account the evolution of  $H_E$  with the pristine O content for the annealed samples where, upon a certain O content (i.e., 15%),  $H_E$  decreases until reach a steady state value as it happens in FM/AFM bilayers as a function of the AFM thickness,<sup>3,27,29</sup> it seems plausible to assume that, while the Co counterpart of the samples implanted to a fluence above  $1 \times 10^{17}$  ions/cm<sup>2</sup> (15% O) might be rather similar in size, the AFM CoO counterparts are thicker in samples with higher pristine O content, resembling the universal-like dependence of the exchange bias shift on the amount of pristine O content.<sup>17</sup> Conversely, the coercivity shows a monotonic increase with the pristine amount of O (Fig. 2(e)). This could be correlated not only to an increased density of defects for samples implanted at higher fluences (i.e., slightly less efficient structural recovery by annealing) but also to a diminution of the exchange interactions between Co grains, which usually has a detrimental effect on coercivity.<sup>16</sup> This is consistent with the phase separation in the O-implanted layer which yields Co rich pure areas embedded in a structurally well-defined CoO.

As can be seen in Fig. 3, annealing leads to samples with significantly larger blocking temperatures ( $T_B$ ) than those of the as-implanted films.<sup>17,19</sup> Specifically, while the annealed samples containing pristine O contents of 5%, 8%, and 15% exhibit  $T_B$  values of around 225, 235, and 255 K, respectively, the rest of the samples show blocking temperatures close to that of the Néel temperature of bulk CoO (i.e., 290 K).<sup>30</sup> This is in concordance with the structural and magnetic characterization since annealing results in the formation (specially in samples with higher pristine O content) of thicker and more stoichiometric CoO counterparts with higher magnetic anisotropy, which are less prone to size effects. Since usually  $T_B$  is highly affected (i.e., lowered) by deviations in stoichiometry of the AFM,<sup>30</sup> the high  $T_B$  values of the different samples confirm that the formed CoO is rather well-defined from a structural point of view with

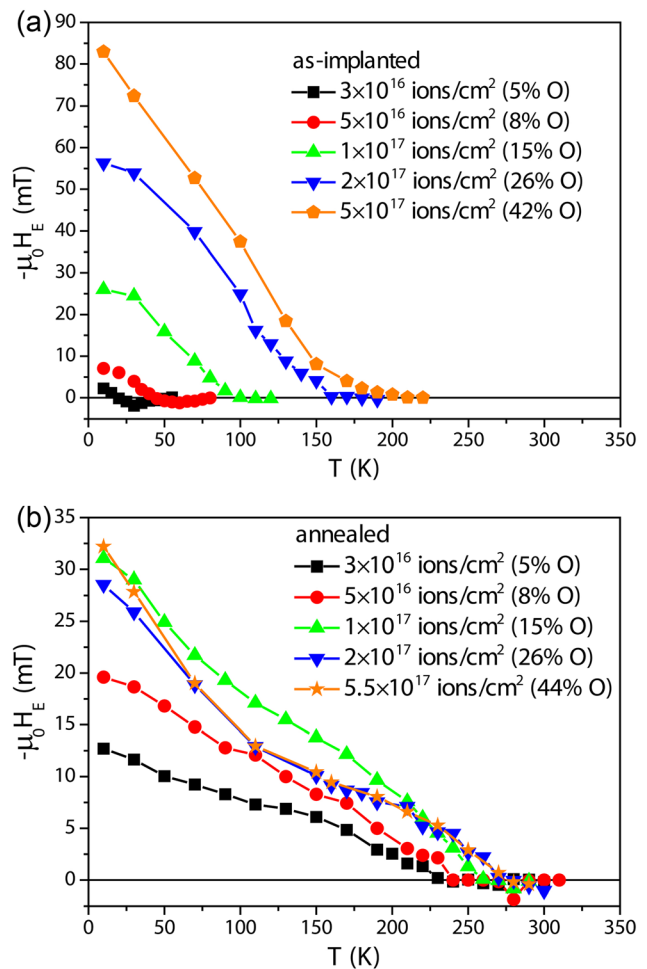


FIG. 3. Temperature dependence of the exchange bias shift,  $H_E$ , for the as-implanted (a) and annealed samples (b). The lines are connections between the data.

minimized composition deficiencies. This is further confirmed by the decreased positive exchange bias<sup>31,32</sup> close to the blocking temperature of samples implanted at low fluence ( $3 \times 10^{16}$  and  $5 \times 10^{16}$  ions/cm<sup>2</sup>) and annealed, indicating an increased AFM magnetic anisotropy of the formed CoO. In addition, the temperature dependence of the  $H_E$  of the annealed samples (Fig. 3(b)) exhibits a more linear behavior than that of the as-implanted ones (Fig. 3(a)), confirming the rather bilayer-like behavior of these granular systems after annealing and, thus, evidencing a lowered number of FM/AFM interfaces.<sup>33</sup>

#### IV. CONCLUSIONS

The response of O-implanted Co thin films with a uniform O-depth distribution to thermal activation effects has been addressed. The annealing results in a pronounced separation of Co and O, leaving highly pure Co areas embedded in a structurally relaxed and compositionally well-defined CoO matrix with increased magnetocrystalline anisotropy. This leads to a faster stabilization of training and to reduced relative training effects. After annealing, the amount of CoO becomes drastically reduced due to O migration away from the Co layer. This results in a lowered number of FM/AFM interfaces and, thus, in considerably decreased exchange bias

shifts. Remarkably, the dependence of the exchange bias shift on the implanted O content for the annealed samples resembles that of the dependence on the AFM thickness in FM/AFM systems, suggesting that, while the Co constituent remains rather constant in size in samples implanted to a fluence above  $1 \times 10^{17}$  ions/cm<sup>2</sup> (15% O), the AFM CoO counterparts become thicker in samples with higher pristine O content. Annealing also leads to samples with significantly higher  $T_B$  than those of the as-implanted samples which, for samples implanted above  $1 \times 10^{17}$  ions/cm<sup>2</sup> and annealed, are close to the Néel temperature of bulk CoO. This shows that the exchange bias properties of Co-CoO systems prepared by ion implantation can be tuned by controllably modifying the local microstructure through annealing procedures.

## ACKNOWLEDGMENTS

This work was financed by the Research Foundation - Flanders (FWO) and the KU Leuven Concerted Action (GOA/09/006 and GOA/14/007) programs. We thank the European Synchrotron Radiation Facility (ESRF, proposal HC-1012, BM20 beamline) for the allocation of synchrotron radiation beam time and C. Bächtz for the assistance during the experiments. E.M. and L.M.C.P. thank the FWO for financial support. T.D. thanks the CNPq agency (Project No. 245897/2012-7) for financial support. The authors thank J. Nogués for fruitful discussions.

<sup>1</sup>J. Nogués and I. K. Schuller, *J. Magn. Magn. Mater.* **192**, 203 (1999).

<sup>2</sup>A. E. Berkowitz and K. Takano, *J. Magn. Magn. Mater.* **200**, 552 (1999).

<sup>3</sup>J. Nogués, J. Sort, V. Langlais, V. Skumryev, S. Suriñach, J. S. Muñoz, and M. D. Baró, *Phys. Rep.* **422**, 65 (2005).

<sup>4</sup>F. Radu and H. Zabel, "Exchange bias effect of ferro-/antiferromagnetic heterostructures," *Springer Tracts Mod. Phys.* **227**, 97 (2007).

<sup>5</sup>S. Brück, G. Schütz, E. Goering, X. S. Ji, and K. M. Krishnan, *Phys. Rev. Lett.* **101**, 126402 (2008).

<sup>6</sup>J. Geshev, T. Dias, S. Nicolodi, R. Cichelero, A. Harres, J. J. S. Acuña, L. G. Pereira, J. E. Schmidt, C. Deranlot, and F. Petroff, *J. Phys. D: Appl. Phys.* **44**, 095002 (2011).

<sup>7</sup>Ch. Binek, *Phys. Rev. B* **70**, 014421 (2004).

<sup>8</sup>A. Harres and J. Geshev, *J. Phys.: Condens. Matter* **23**, 216003 (2011).

<sup>9</sup>S. R. Ali, M. R. Ghadimi, M. Fecioru-Morariu, B. Beschoten, and G. Güntherodt, *Phys. Rev. B* **85**, 012404 (2012).

<sup>10</sup>A. Hoffmann, *Phys. Rev. Lett.* **93**, 097203 (2004).

<sup>11</sup>S. Brems, K. Temst, and C. Van Haesendonck, *Phys. Rev. Lett.* **99**, 067201 (2007).

<sup>12</sup>B. Dieny, V. S. Speriosu, S. S. P. Parkin, B. A. Gurney, D. R. Wilhoit, and D. Mauri, *Phys. Rev. B* **43**, 1297 (1991).

<sup>13</sup>A. Moser, K. Takano, D. T. Margulies, M. Albrecht, Y. Sonobe, Y. Ikeda, S. Sun, and E. E. Fullerton, *J. Phys. D: Appl. Phys.* **35**, R157 (2002).

<sup>14</sup>M. Gruyters and D. Riegel, *Phys. Rev. B* **63**, 052401 (2000).

<sup>15</sup>J. Demeter, J. Meersschaut, F. Almeida, S. Brems, C. Van Haesendonck, A. Teichert, R. Steitz, K. Temst, and A. Vantomme, *Appl. Phys. Lett.* **96**, 132503 (2010).

<sup>16</sup>J. Demeter, E. Menéndez, K. Temst, and A. Vantomme, *J. Appl. Phys.* **110**, 123902 (2011).

<sup>17</sup>E. Menéndez, J. Demeter, J. Van Eyken, E. Jedryka, M. Wójcik, P. Nawrocki, J. F. Lopez-Barbera, J. Nogués, A. Vantomme, and K. Temst, *ACS Appl. Mater. Interfaces* **5**, 10118 (2013).

<sup>18</sup>J. Demeter, E. Menéndez, A. Schrauwen, A. Teichert, R. Steitz, S. Vandezande, A. R. Wildes, W. Vandervorst, K. Temst, and A. Vantomme, *J. Phys. D: Appl. Phys.* **45**, 405004 (2012).

<sup>19</sup>E. Menéndez, T. Dias, J. Geshev, J. F. Lopez-Barbera, J. Nogués, R. Steitz, B. J. Kirby, J. A. Borchers, L. M. C. Pereira, A. Vantomme, and K. Temst, "Interdependence between training and magnetization reversal in granular Co-CoO exchange bias systems," *Phys. Rev. B* (in press, 2014).

<sup>20</sup>F. J. Toole and F. M. G. Johnson, *J. Phys. Chem.* **37**, 331 (1933).

<sup>21</sup>See <http://icstd.fiz-karlsruhe.de/icstd/> for a database for inorganic crystal structures; accessed 15 November 2013.

<sup>22</sup>H. Fulara, S. Chaudhary, and S. C. Kashyap, *Appl. Phys. Lett.* **101**, 142408 (2012).

<sup>23</sup>M. S. Lund and C. Leighton, *Phys. Rev. B* **76**, 104433 (2007).

<sup>24</sup>T. Gredig, I. N. Krivorotov, and E. Dan Dahlberg, *Phys. Rev. B* **74**, 094431 (2006).

<sup>25</sup>T. Gredig, I. N. Krivorotov, and E. Dan Dahlberg, *J. Appl. Phys.* **91**, 7760 (2002).

<sup>26</sup>J. Keller, P. Miltényi, B. Beschoten, G. Güntherodt, U. Nowak, and K. D. Usadel, *Phys. Rev. B* **66**, 014431 (2002).

<sup>27</sup>R. Jungblut, R. Coehoorn, M. Johnson, J. aan de Stegge, and A. Reinders, *J. Appl. Phys.* **75**, 6659 (1994).

<sup>28</sup>M. Ali, C. H. Marrows, M. Al-Jawad, B. J. Hickey, A. Misra, U. Nowak, and K. D. Usadel, *Phys. Rev. B* **68**, 214420 (2003).

<sup>29</sup>X. S. Liu, B. X. Gu, W. Zhong, H. Y. Jiang, and Y. W. Du, *Appl. Phys. A: Mater. Sci. Process.* **77**, 673 (2003).

<sup>30</sup>G. Nowak, A. Remhof, F. Radu, A. Nefedov, H.-W. Becker, and H. Zabel, *Phys. Rev. B* **75**, 174405 (2007).

<sup>31</sup>B. T. Gredig, I. N. Krivorotov, P. Eames, and E. Dan Dahlberg, *Appl. Phys. Lett.* **81**, 1270 (2002).

<sup>32</sup>C. Prados, E. Pina, A. Hernando, and A. Montone, *J. Phys.: Condens. Matter* **14**, 10063 (2002).

<sup>33</sup>F. Radu, M. Etzkorn, R. Siebrecht, T. Schmitte, K. Westerholt, and H. Zabel, *Phys. Rev. B* **67**, 134409 (2003).